

## Disk-Instability Model: Introduction

---

**Shin Mineshige<sup>a,\*</sup>**

*Kyoto University,*

*Oiwake-cho, Sakyo-ku, Kyoto, Japan*

*E-mail: [shm@kustastro.kyoto-u.ac.jp](mailto:shm@kustastro.kyoto-u.ac.jp)*

The research history of accretion disks and flow is overviewed with special attention to the impacts of the disk-instability model. The standard disk model was built under (radially) one-dimensional approximation and had some success in describing the basic properties of the accreting systems. However, this model is known to break down under several circumstances. Alternative models have been proposed as an extension of the standard disk model. The disk-instability model is one of such attempts and is unique in providing us with rich information regarding the time-dependent properties of accretion disks. We first show the necessity of solving the multi-zone vertical structure to incorporate convective energy transport, which is required for producing S-shaped equilibrium curves. We next introduce two-zone models for disk-corona structure and discuss how to reproduce observational properties. We finally discuss the time-dependent properties of accretion disks undergoing dwarf-nova type disk instability and its applications to the X-ray binaries.

*87th Fujihara Seminar: The 50th Anniversary Workshop of the Disk Instability Model in Compact Binary Stars (DIM50TH2025)  
22-26 September 2025  
Tomakomai, Japan*

---

\*Speaker

## 1. Introduction – Brief History of Accretion Disk/Flow Research

This paper aims to provide a basic background on the subjects discussed in this volume to those unfamiliar with the research history of accretion disks and flow. We wish to emphasize the impact of the disk-instability model, pioneered by Osaki (Ref. [1]), on accretion disk/flow studies.

Let us begin with a brief history of accretion disk/flow studies in the last century. Extensive studies of accretion disks and flows started with the discovery of X-ray stars in the 1960s. Soon after that, attempts to construct disk models were initiated by several authors (e.g., Zel'dovich, Salpeter, Lynden-Bell, Rees, Pringle ...). The standard SS (Shakura-Sunyaev) disk model, which was proposed by Ref. [2], is a steady, radially one-dimensional (1-D) disk model. In the vertical direction, a one-zone approximation is adopted. Along the same line, extension of the SS model was proposed (see Ref. [3] and references therein). These studies have been elaborated by multi-dimensional numerical simulations in the 21st century.

There is another line of accretion disk studies, the disk-instability model, developed from the 1970s by several authors (e.g., Osaki, Hoshi, Meyer, Meyer-Hofmeister, Smak, Lin, Cannizzo, Wheeler, etc.). Notably, this is a time-dependent, radially multi-zone, and vertically multi-zone model. The so-called limit-cycle instability model for dwarf-nova (DN) outbursts and for X-ray nova (XN) eruptions is successful. This model (hereafter, the DN-type instability model) could explain the basic light curves and other properties of the observations of DNe and XNe. The direct, quantitative comparison between the time-varying observational data and the time-dependent theory is now made feasible with this model.

Another type of the limit-cycle instability model, the radiation pressure-driven instability model, was proposed after the success of the DN-type one. This model may explain the repetitive bursts of the microquasar GRS1915+105. Other types of disk instabilities (such as pulsational and tidal instabilities) have also been discussed in relation to various types of light variations (e.g., quasi-periodic oscillations) shown by cataclysmic variables (CVs) and X-ray binaries (XBs).

In the following sections, we focus on the DN-type limit cycle instability and discuss how its model enriches our view of accretion flow. In section 2, we overview the 1-D disk/flow models: the standard disk model, the hot accretion flow model (ADAF/RIAF...), and the super-Eddington (slim) disk model. In section 3, we describe the vertical disk structure in two distinct contexts: a multi-zone model for convective energy transport and two-zone models for disk-corona structure. In section 4, we introduce the time-dependent equations of accretion flow and examine how accretion disks exhibit time variations.

## 2. The standard disk model and its extensions

We first overview the classical (radially 1-D) disk models in this section.

### 2.1 Standard (SS) disk model

The basics of the standard accretion disk model is found in its energetics. From the combinations of the basic equations of viscous disks (see Table 1), we finally obtain

$$Q_{\text{rad}}^-(r) = Q_{\text{vis}}^+(r) = Q_{\text{grav}}^+(r). \quad (1)$$

Here,  $Q_{\text{rad}}^-$ ,  $Q_{\text{vis}}^+$ ,  $Q_{\text{grav}}^+$  are the radiative cooling rate, viscous heating rate, and the release rate of the gravitation potential energy, respectively, at a radius  $r$  for a given mass accretion rate,  $\dot{M}$ .

<b>Standard disk equations</b> (Newtonian version)	
<b>mass conservation</b>	$\dot{M} = -2\pi r v_r \Sigma$
<b>Kepler rotation</b>	$\Omega^2 = \Omega_K^2 \equiv \frac{GM}{r^3}$
<b>ang. mom. cons.</b>	$v_{\text{vis}} \Sigma = \frac{\dot{M}}{3\pi} \left(1 - \sqrt{\frac{r_{\text{in}}}{r}}\right)$
<b>energy equation</b>	$Q_{\text{vis}}^+ = Q_{\text{rad}}^-$
<b>alpha viscosity</b>	$v_{\text{vis}} = \alpha c_s H$
<b>hydrostatic balance</b>	$H = c_s / \Omega$ ; $c_s = \sqrt{P/\rho}$

**Table 1:** Basic equations of the standard (SS) disk model. Here,  $v_r$ ,  $\Omega$ ,  $H$ , and  $c_s$  are radial velocity of gas, angular frequency, disk height, and sound velocity, respectively (for other symbols, see text).

If we explicitly write down each term of Eq. (1), we have

$$F(r) = (9/8) v_{\text{vis}} \Sigma \Omega_K^2 = (3GM\dot{M}/8\pi r^3) \left(1 - \sqrt{r_{\text{in}}/r}\right), \quad (2)$$

where  $F(r)$  is the emergent flux from unit surface area of the disk,  $v_{\text{vis}}$  is the kinematic viscosity,  $\Sigma$  is surface density,  $\Omega_K (= \sqrt{GM/r^3})$  is the Keplerian angular frequency,  $G$  is the gravitational constant,  $M$  is the mass of a compact object, and  $r_{\text{in}}$  is the inner edge of the disk, respectively.

This equation says that gravitational potential energy (term on the right-hand side) is converted to thermal energy via viscous processes (the middle term) and finally to radiation energy (term on the left-hand side) via blackbody radiation. In other words, this equation demonstrates that the gravitational energy of accreting gas is *efficiently* converted to radiation energy. The total luminosity,  $L_{\text{disk}}$ , is then calculated by

$$L_{\text{disk}} = \int 4\pi r^2 2F(r) dr = GMM\dot{M}/(2 r_{\text{in}}). \quad (3)$$

That is, the smaller the radius of the inner disk edge is, the larger the power the disk can emit.

## 2.2 Extension of the SS disk model

The standard SS disk model is very successful, but this is not the end of the story. It was already recognized in the 1970s that black hole binaries (BHBs), such as Cyg X-1, show two distinct spectral states: high/soft state and low/hard state. The former can be well understood in the framework of the standard disk model, but the latter cannot. That is, the standard disk model is not enough to explain a variety of observations.

Soon after its establishment, the limitations of the SS disk model were known in three distinct situations, at least. First of all, the standard disk model breaks down at low luminosities; it cannot explain wide-band (radio to hard X-ray and gamma-ray) emission. This led to the idea of ADAF (advection-dominated accretion flow) or RIAF (radiatively inefficient accretion flow, see a review by Ref. [3], chapter 9, and references therein). It is later shown that the low/hard state of Cyg X-1 can be explained by the ADAF/RIAF model.

Second, the SS disk model breaks down at high luminosities, close to the Eddington luminosity,  $L_{\text{Edd}}$ . In fact, this model cannot adequately describe radiation-matter interaction, which becomes essential when the disk luminosity is comparable to  $L_{\text{Edd}}$ . This led to the idea of the slim disk model, or the super-Eddington accretion flow (see a review by Ref. [3], chapter 10, and references therein).

To generalize the standard disk model, we need to relax some of the basic assumptions made in the standard disk model (see Table 1). We thus allow the non-Keplerian rotation and need to introduce the advective energy transport term, which describes entropy transport accompanied by accreting gas. Now the energy equation reads,

$$Q_{\text{adv}}^- \equiv \frac{v_r}{2} \Sigma T \frac{ds}{dr} = Q_{\text{vis}}^+ - Q_{\text{rad}}^- \quad (4)$$

Here, the term on the left-hand side represents the advective cooling. To understand why it is called “cooling,” we need to distinguish between two frames. If we follow the accretion motion of gas, there is practically *no cooling* because of low radiation efficiency. If we stand in and see a specific region (i.e., annulus) with a fixed radius, we notice that low-entropy ( $s$ ) gas comes in (from the adjacent outer annulus) and high-entropy gas goes out (to the adjacent inner annulus). That is, entropy produced by viscous processes in that annulus is carried away by gas moving inward. This effect is nothing but the advective cooling.

Finally, the SS disk model breaks down at low temperatures below 10,000 K. This is because partial ionization/recombination of hydrogen and helium, which significantly affect the radiative cooling term, are not considered in the SS model. This led to the construction of the DN-type disk instability model (see sec. 3-4).

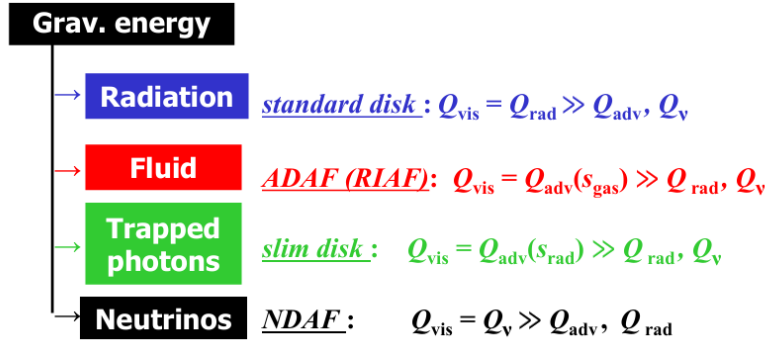


**Figure 1:** Schematic explanations of various disk models.

In Figure 1, we summarize the various (1-D) disk models. We can distinguish them in terms of the final destination of the input energy; gravitational energy goes to radiation, fluid, trapped photons, and neutrinos in the standard disk, ADAF (or RIAF), slim disk, and NDAF (neutrino-dominated accretion flow). The last one appears at extremely super-Eddington accretion rates.

For understanding the relationship between these disk models, it is very useful to use the thermal equilibrium curves. In Figure 2, we plot the loci of the thermal equilibrium solutions, in which the heating rate,  $Q^+$ , is balanced with the cooling rate,  $Q^-$ , on the  $\log \Sigma$ -  $\log \dot{M}$  plane (see, e.g., Ref. [4]). The NDAF solutions are omitted there. Note that the right (or left) part of the curves corresponds to the optically thick (thin) branches of the solutions. The regimes, in which the two types of limit-cycle instabilities take place (sec. 4), are also indicated in this figure.

### 3. Vertical disk structure

In the (radially) 1-D models, the vertical distribution of each physical quantity (such as density and temperature) is represented by only one value. To properly calculate the S-shaped thermal equilibrium curve, however, we need to integrate the vertical disk structure (sec. 3.1 and 3.2). Another issue is the existence of a high-temperature disk corona (sec. 3.3 and 3.4).

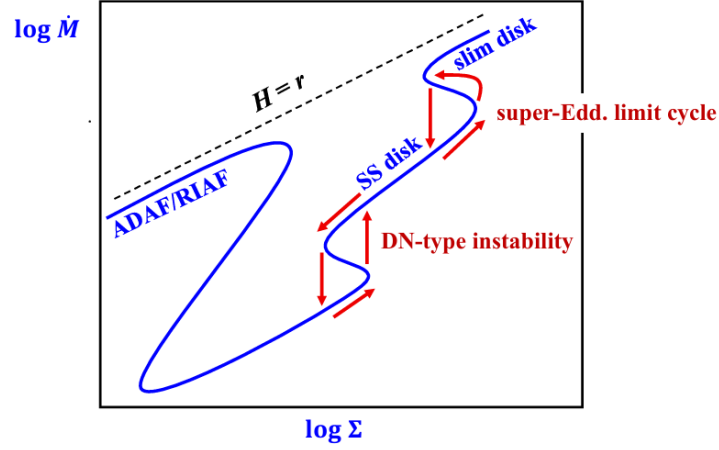


**Figure 2:** Thermal equilibrium curves of distinct types of accretion disks on the  $\log \Sigma$ -  $\log \dot{M}$  plane.

### 3.1 Multi-zone vertical disk structure

In the early 1980s, the vertical disk structure of the cool disks (as found in the quiescence of DNs) was intensively investigated. The basic equations for describing the disk's vertical structure look quite similar to those for the radial stellar structure. Let us compare these two sets of basic equations in Table 2. Both of them are comprised of the equation of mass conservation, the hydrostatic balance, the energy flux equation, and the energy equation.

	Stellar interior structure	Vertical disk structure
mass conservation	$\frac{dM_r}{dr} = 4\pi r^2 \rho$	$\frac{d\Sigma_z}{dz} = 2\rho$
hydrostatic balance	$\frac{dP}{dr} = -\rho \frac{GM_r}{r^2}$	$\frac{dP}{dz} = -\rho g_z (= -\rho \Omega^2 z)$
energy flux	$L_r = 4\pi r^2 (F_{\text{rad}} + F_{\text{conv}})$	$F_z = F_{\text{rad}} + F_{\text{conv}}$
energy equation	$\epsilon = \frac{dL_r}{dM_r}$	$q_{\text{vis}} = \frac{dF_z}{dz}$

**Table 2:** Basic equations for the stellar interior structure and the vertical disk structure.

Here,  $M_r(r) \equiv \int_0^r 4\pi r^2 \rho(r) dr$ ,  $\Sigma_z(r) \equiv \int_0^z 2\rho(r, z) dz$ ,  $F_{\text{rad}}$ ,  $F_{\text{conv}}$ ,  $\epsilon$ , and  $q_{\text{vis}}$  are mass coordinate, surface-density coordinate, radiative energy flux, convective energy flux, nuclear energy generation rate, and viscous heating rate, respectively. Other symbols have their usual meanings. Note that the spherical coordinates,  $(r, \theta, \varphi)$ , are used for the stellar structure, while the cylindrical coordinates,  $(r, \varphi, z)$ , are adopted for the disk structure.

Some differences are found in the energy equation, since nuclear energy generation is available locally, whereas viscous heating is available everywhere within the disk. This is one of the reasons why vertical integration is essential, but there is another, even more important reason for vertical integration. We need to solve multi-layer structures because convective energy transport overcomes radiative energy transport in certain cases, both in stars and in disks.

It is well known that convective energy transport dominates radiative one in the outer cool zone of low-mass stars, in which temperature gets below  $10^4$  K, and in the inner hot zone of the

high-mass star. Similarly, convection is important in cool disks with temperatures below  $10^4$  K, and in hot disks, in which radiation pressure dominates. Recall that the temperature of the quiescent disk in dwarf novae is low,  $T < 10^4$  K, so that hydrogen and helium should be partially ionized, a condition for convective instability. [This is because the convective instability criterion,  $\nabla \equiv d \ln T / d \ln P > \nabla_{\text{ad}} = (\gamma - 1) / \gamma$ , is easily satisfied in the partially ionization zone, where the adiabatic index  $\gamma$  is close to unity.] In order to incorporate convective energy transport, we need vertical integration of the disk structure.

### 3.2 S-shaped equilibrium curves

Figure 3 is the famous S-shaped thermal equilibrium curve. As is well known, the disks on the upper and lower branches are thermally stable, whereas those on the middle branch are unstable. This can be easily confirmed in the following way. Suppose that the initial disk is on the lower branch of the thermal equilibrium solutions,  $Q^+ = Q^-$ . When we slightly heat up the disk, it will then enter the regime of  $Q^+ < Q^-$ , thereby disk temperature being reduced. The disk will return to the original position, meaning thermal stability. (Note that  $\dot{M}$  decreases as the disk temperature decreases.) If the disk is on the middle branch, conversely, a temperature increase promotes a further increase of temperature, causing thermal runaway (and an upward transition to the upper branch), meaning thermal instability. In short, the instability condition is

$$(dQ^+ / dT)_{\Sigma} > (dQ^- / dT)_{\Sigma} \quad (5)$$

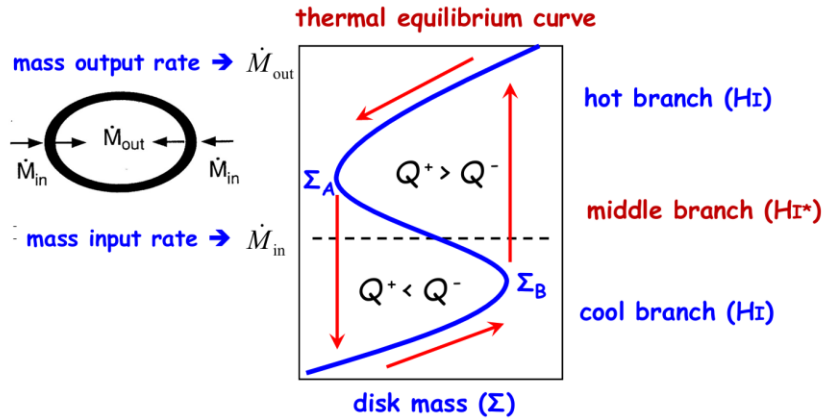


**Figure 3:** S-shaped thermal equilibrium curve. Limit-cycle type oscillations occur when the mass input rate into the disk corresponds to the mass output rate on the middle branch.

When the mass input rate corresponds to that of the middle branch, therefore, limit-cycles between the hot stable branch and the cool stable branch are produced (see Fig. 3). We wish to stress that this S-shaped curve is obtained only when vertical integration is made. Why? Because energy transport within the disk on the middle branch is dominated by convective energy transport, and not by radiative energy transport.

### 3.3 Two-zone disk-corona models

The next issue is the construction of a disk-corona model. The co-existence of hot and cool plasmas is indicated by the discovery of the reflection component. Here, by hot (or cool) plasmas, we mean that metals, such as Fe, are fully ionized (partially ionized or neutral).

There are (at least) three possibilities as to the geometrical relationship of the hot and cool plasmas (see Fig. 4). In (a) horizontal separation, a hot inner torus is surrounded by a cool disk, while in (b) vertical separation, a cool disk is sandwiched by hot coronae. The mixed case (c) is sometimes called as “truncated disk” case (see, e.g., Ref. [5] for a review). In any case, the most essential is how to produce hot plasmas from cool disk material.

An evaporation model of disk material was proposed by Ref. [6] in analogy with the solar corona. It is known that hot coronae (with a temperature of  $\sim 10^6$  K) are formed above the solar photosphere (with a temperature of  $\sim 6000$  K). Photospheric cool material is heated via thermal conduction process and evaporates into the hot corona. Similarly, a hot disk corona seems to be formed above the disk photosphere in AGN and X-ray binaries (see Fig. 4).

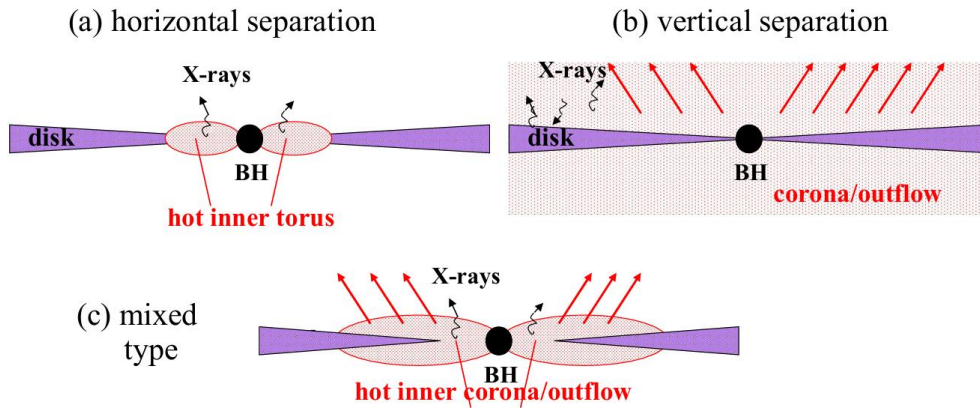


**Figure 4:** Three types of configurations for the co-existence of hot and cool plasmas.

Let us try to understand how to form hot coronae by using the two-zone disk-corona model. Here, we make a very important assumption (Ref. [7]); that is, we assume that a substantial fraction ( $f$ ) of the total energy input,  $Q_{\text{tot}}^+$  ( $= Q_{\text{grav}}^+$ ), is dissipated within a corona (see Fig. 5). Here, we require the value of  $f$  to be relatively large, close to unity.

This is important, since otherwise disk coronae are too much Compton-cooled to maintain hot temperature. We can thus build up two equations: one is the energy balance in disk body

$$[1 - (f/2)] Q_{\text{tot}}^+ = F_{\text{soft}}; \quad F_{\text{soft}} = \sigma T_{\text{disk}}^4 \quad (6)$$

with  $T_{\text{disk}}$  being the surface temperature of the disk body. Here, the term of  $(f/2)$  on the left-hand-side means that about a half of hard photons created within a corona goes outward, while the remaining half returns and heat up the disk plasmas. Another is the energy balance in the disk corona. Assuming inverse-Compton cooling of the corona by  $F_{\text{soft}}$ , we have

$$f Q_{\text{tot}}^+ = y F_{\text{soft}}; \quad y \equiv (4kT_{\text{cor}}/m_e c^2) (\tau_{\text{es}}^2 + \tau_{\text{es}}) \quad (7)$$

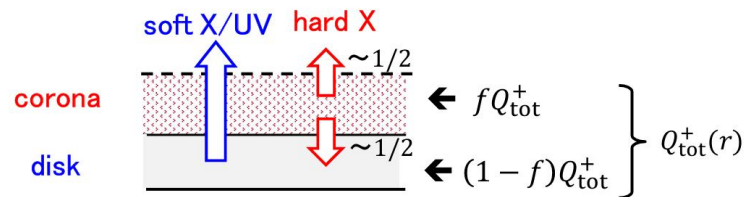


**Figure 5:** Schematic figure explaining the energy flow in a two-zone disk-corona model

with  $y$ ,  $k$ ,  $T_{\text{cor}}$ , and  $\tau_{\text{es}}$  being the Compton  $y$ -parameter, the Boltzmann constant, coronal temperature, and the Thomson optical depth of the corona, respectively. The combinations of these two equations lead to a simple relation,

$$y = 2f/(2 - f). \quad (8)$$

We thus find  $f = 2/3$  for  $y = 1$  (or  $f = 1$  for  $y = 2$ ). Note that the values of  $y = 1 - 2$  are rough what are obtained by the spectral fitting. Note that we find  $kT_{\text{cor}} \sim 100$  keV for the Thomson optical depth of  $\tau_{\text{es}} \sim 1$  from the definition of  $y$  [see Eq. (7)].

### 3.4 Hot corona and warm corona

Recently, the existence of warm corona (with  $kT_{\text{cor}} \sim 0.1$  keV or so) is indicated by the observations of at least some AGNs. The X-ray spectra of Sy 1 galaxies are composed of the big blue bump in the UV and a power-law component with an exponential cutoff in the hard X-ray bands. The former can be interpreted as the emission of a standard-type disk, while the latter can be described by a hot corona. In addition, we know the ubiquitous existence of soft X-ray excess below the photon energy of  $\sim 2$  keV.

Interestingly, the soft X-ray excess component seems to disappear when the AGN luminosity drops below a certain level. Noda & Done (Ref. [8]), for example, reported the variations of spectral components of a changing-look (CL) AGN, Mrk 1018, which exhibited rapid luminosity variations, from  $L/L_E = 0.08$  to  $0.006$  in 8 years. The variation amplitude is more than one order of magnitude. They attempted spectral decompositions, finding three major spectral components: the big blue bump, the soft X-ray excess, and the cut-off power-law component in the hard X-rays. Interestingly, the soft X-ray excess disappeared at low luminosities, below a few percent of the Eddington ( $L_E$ ). The broad-line region also disappeared then.

A question then arises: what is the origin of the soft X-ray excess? One of the most promising models is the warm corona model (e.g., Ref. [9]). The warm corona means a corona with a temperature of  $T \sim 10^6$  K (or  $kT \sim 0.1$  keV) in contrast with a hot corona with a temperature of  $T \sim 10^9$  K (or  $kT \sim 100$  keV). The properties of the warm hot coronae are summarized in Ref. [9]. Since the photon index is related to the Compton  $y$  parameter in unsaturated Compton spectra, similar photon indices indicate a similar  $y$  parameter, roughly  $y \sim 1$ .

Recall that this feature is also found for hot coronae. This is not surprising, since the layer of  $y \sim 1$  in a Compton-dominated atmosphere corresponds to the photosphere in an absorption-dominated atmosphere in the sense that photons traveling away to observers carry information of that layer. Then, what makes the difference between hot and warm coronae? The answer is the value of the Thomson optical depth; it is  $\tau_{\text{es}} \sim 1$  in hot coronae, while  $\tau_{\text{es}} \sim 30$  in warm coronae. This is obvious from the definition of the  $y$ -parameter [see Eq. (7)].

Then, the next question arises: what determines the value of  $\tau_{\text{es}} \sim 30$  in warm coronae? In our model (Ref. [10]) we assume that the depth of the warm corona is set by the effective optical depth of  $\tau_{\text{eff}} = \sqrt{3\tau_{\text{es}}\tau_{\text{abs}}} \sim 1$ , where  $\tau_{\text{abs}}$  is the absorption optical depth. (The effective optical depth represents the practical absorption optical depth in a scattering-dominated atmosphere.) With this model, we can roughly reproduce the temperature of a warm corona to be greater than that of soft (seed) photons to be Compton up-scattered by a factor of 3 or so.

## 4. Time-dependent behavior

The final subject is the time-dependent properties of accretion disks undergoing instabilities.

#### 4.1 Outbursts and erupting phenomena

Dwarf novae are known to show repetitive outbursts with amplitudes of 2 ~ 5 mag. The outburst interval is typically several tens of days. Similar types of repetitive bursts, but on much longer timescales, are known in X-ray binaries containing black holes. Fig. 6 shows the X-ray light curves of black-hole X-ray novae discovered by the Ginga satellite. Rapid rise (on a few days) and exponential decay (over several months) are their common characteristics. Moreover, the spectral state transitions from the low/hard state to the high/soft state, and again to the low/hard state with a hysteresis are commonly observed. The burst interval is several tens of years. Much longer timescales of light variations in black-hole XNe can be understood, since the viscous time-scale is proportional to  $M^{1/2}R_{\text{disk}}^{1/2}$  (see, e.g., Ref. [3], chapter 5). **This is, however, not sufficient to explain the large differences between DNe and XNe. Another factor is irradiation effects during the outbursts, which help to prolong the burst duration (see sec. 4.3).**

We need to make remarks on the disk instability model for XNe. When we try to apply the DN-type instability model to XBs, we are confronted with two major issues. The first issue is that much larger accretion disks are in XBs. To produce large amplitude X-ray variations, the cooling front (which appears during a downward transition from the hot branch to the cool branch) should propagate down to the innermost region of the disk. A big question is, therefore, can the cooling front propagate from  $r \sim 10^5 r_S$  all the way down to  $\sim 3 r_S$ ? Here,  $r_S = 2GM/c^2$  is the Schwarzschild radius.

The second issue is the irradiation effects of central radiation. Radiation from the inner hot region is so intense that the gas in the outer region could be significantly heated up, thereby suppressing the DN-type instability. So the question is, is the temperature of the quiescent disk in XNe kept well below  $10^4$  K?

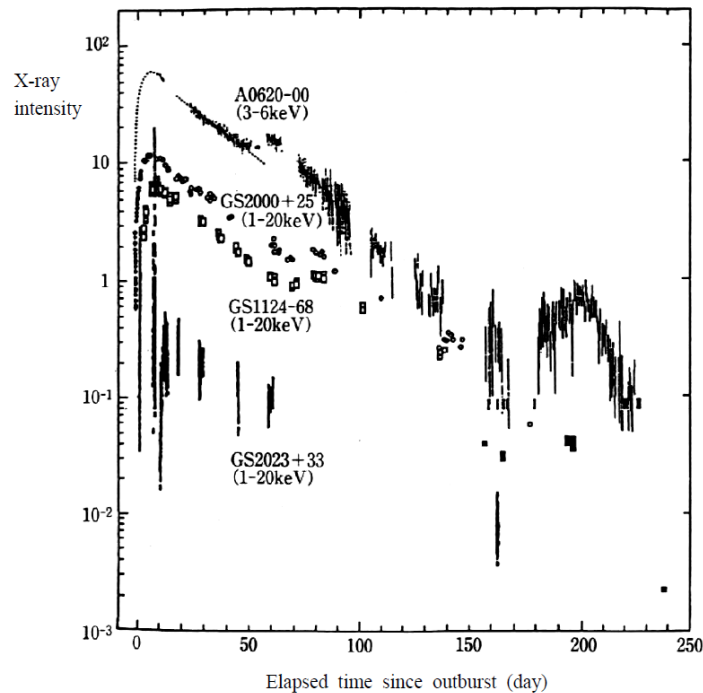


**Figure 6:** X-ray intensity variations of some black hole X-ray novae (Ref. [11]).

## 4.2 Condition for large-amplitude variations

The first issue is regarding the propagation of the cooling front. The important fact is that the disk evolves in a self-similar fashion on the  $\log r$ - $\log \Sigma$  plane. This means, if the cooling front can propagate over a certain range of radial distance, it will propagate until it reaches the innermost region. Then, what is the condition for the cooling front to propagate inward?

The answer is that the angular momentum contained in the outer part of the inner hot zone should be transferred to the transition zone. This condition is expressed in terms of  $\Sigma_B/\Sigma_A$ , where  $\Sigma_A$  and  $\Sigma_B$  denote the values of surface density at the upper and lower critical points (see Fig. 3). Ref. [12] inspected this condition, finding that  $\Sigma_B/\Sigma_A > 2$  for the cooling front to propagate continuously inward. (Otherwise, an inward cooling front should be reflected to become an outgoing heating wave.) This condition is satisfied only when we assign a lower  $\alpha$  value in the cool branch and a higher value in the hot branch;  $\alpha_{\text{cool}} < \alpha_{\text{hot}}$  (see Hirose in this volume).

## 4.3 Irradiation effects

The second issue is the effects of irradiation. Ref. [13] solved the vertical disk structure under irradiation effects, finding the condition for the disk-instability model to survive to be that the irradiation temperature should be below 4500 K (see Fig. 7). This is, in turn, expressed in terms of the X-ray luminosity during the quiescence;  $L_Q < 10^{34}$  erg s<sup>-1</sup>. This condition seems to be satisfied by the X-ray observations. (Note, however, that irradiation effects should be important in the outburst phase.)

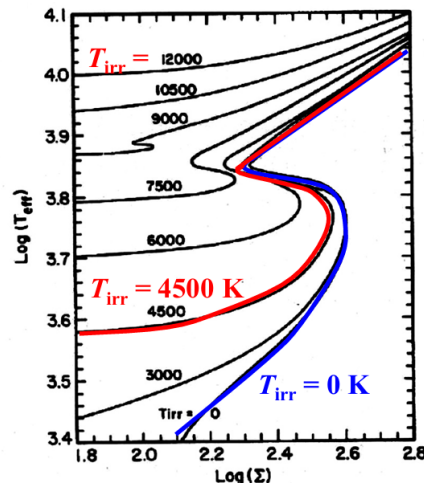


**Figure 7:** Thermal equilibrium curves of irradiated disk (Ref. [13]).

We thus have good reasons to believe that the DN-type disk-instability model can work in black hole XNe. However, there remain issues. Here are examples of the remaining issues in the disk-instability model for black hole X-ray novae.

- Origin of reflare (which are found several tens of days after the peak)
- Origin of third maxima (which appear several months after the peak)
- How to produce GS2023-type bursts? **GS2023-33 exhibits distinct light variation patterns, full of short-term flares, in contrast with the FRED (fast rise and exponential decay) type light curves.**

This is not the complete list of puzzles. It may be interesting to note that some issues (say, item 2) are also discussed in the case of WZ Sge-type dwarf novae. (Note that the third maxima are called “reflares” in the study of WZ Sge.)

#### 4.4 Outstanding issues related to disk instabilities

In the previous subsections, we focused on the DN-type limit-cycle instability. There is another type of limit-cycle instability appearing at much higher luminosities, close to the Eddington luminosity (see Fig. 2). The lower branch is the SS-type disk, while the upper branch is the slim disk. This instability may possibly explain the light variations of the micro-quasar, GRS 1915+105, which shows state transitions between the peak and valley (see relevant papers in this volume).

We wish to make a comment, here, on the stabilizing effects by the disk corona. If a significant fraction of energy is dissipated in a disk corona (sec. 3.3) and if the disk main body is a passive disk (meaning that it is heated externally by the disk corona), a thermal instability in the radiation-pressure dominated regime could be suppressed for the following reason (see Ref. [14]). In a passive disk, we find  $(dQ^+/dT)_\Sigma = 0$ , since the heating rate is independent of the disk temperature, whereas cooling rate (by blackbody radiation) increases with an increase of temperature;  $(dQ^-/dT)_\Sigma > 0$ . We thus have  $(dQ^+/dT)_\Sigma < (dQ^-/dT)_\Sigma$ , condition for thermal stability [see Eq. (5)]. This is, however, a very naive discussion. (For example, we assumed that the corona properties do not respond to a change in the disk condition, but this may not be obvious.) We need more careful analysis.

A variety of disk instabilities, other than those we discussed so far, have been proposed and investigated in past studies. If we relax one of the basic equations for the standard disk model (see Table 1), distinct types of disk instabilities could appear. Deviations from the Keplerian rotation in the radial direction, for example, may excite pulsational instability in the GR potential, or tidal instability in a binary potential. If we relax the condition of hydrostatic balance in the vertical direction, vertical disk oscillations and/or warp may take place. The combination of the mass flow imbalance (between the mass input rate and output rate) and the energy imbalance leads to an onset of the limit-cycle instability, as we have already discussed. Other ingredients, such as disk wind/outflow, magnetic-field activities, and radiation-matter interaction, could trigger distinct types of instabilities. What we discussed in this paper is only the tip of an iceberg. We expect further development of the disk instability studies in the future (see relevant papers in this volume).

#### References

- [1] Y. Osaki, *An Accretion Model for the Outbursts of U Geminorum Stars*, *Publication of Astronomical Society of Japan* **26** (1974) 429.
- [2] N.I. Shakura and R.A. Sunyaev, *Black holes in binary systems. Observational appearance*, *Astronomy and Astrophysics* **24** (1973) 337.
- [3] S. Kato, J. Fukue, S. Mineshige, *Black-Hole Accretion Disks – Towards a New Paradigm*, Kyoto University Press (2008).
- [4] S. Mineshige, and J. H. Wood, *Accretion Disc Atmospheres*, *Monthly Notices of Royal Astronomical Society* **247** (1990) 43

- [5] C. Done, M. Gierliński, A. Kubota, *Modelling the behaviour of accretion flows in X-ray binaries. Everything you always wanted to know about accretion but were afraid to ask*, *Astronomy and Astrophysics Review* **15** (2007) 1
- [6] F. Meyer, E. Meyer-Hofmeister, *Accretion disk evaporation by a coronal siphon flow*. *Astronomy and Astrophysics* **288** (1994) 175
- [7] F. Haardt, L. Maraschi, *A Two-Phase Model for the X-Ray Emission from Seyfert Galaxies*, *Astrophysical Journal* **380** (1991) L51
- [8] H. Noda, C. Done, *Explaining changing-look AGN with state transition triggered by rapid mass accretion rate drop*, *Monthly Notices of Royal Astronomical Society* **480** (2018) 3898
- [9] P.-O. Petrucci, F. Ursini, A. De Rosa, S. Bianchi, M. Cappi, G. Matt, M. Dadina, J. Malzac, *Testing warm Comptonization models for the origin of the soft X-ray excess in AGNs*, *Astronomy and Astrophysics* **611** (2018) 59
- [10] N. Kawanaka, S. Mineshige, *Model of a "Warm Corona" as the origin of the soft X-ray excess of active galactic nuclei*, *Publication of Astronomical Society of Japan* **76** (2024) 306
- [11] Y. Tanaka, in *Ginga Memorial Symposium*, ed. F. Makino & F. Nagase, ISAS (1992) p.19
- [12] S. Mineshige, G. A. Shields, *Accretion Disk Thermal Instability in Galactic Nuclei*, *Astrophysical Journal* **351** (1990) 47
- [13] Y. Tuchman, S. Mineshige, J. C. Wheeler, *Structure and Evolution of Irradiated Accretion Disks. I. Static Thermal Equilibrium Structure*, *Astrophysical Journal* **359** (1990) 164
- [14] S. Mineshige, M. Kusunose, *On the Stability of Irradiated Accretion Disks*, *Publication of Astronomical Society of Japan* **45** (1993) 113